A Bottom-Up Unification of Quantum Mechanics, the Standard Model, Gravity and Cosmology from a Discrete Hypercubic Spacetime Lattice

Bertrand JARRY

souverainbertrand64@gmail.com

February 2026

Abstract

This paper presents a bottom-up unification of quantum mechanics, the Stan-dard Model, gravity, cosmology, and quantum gravity derived from a single minimal structure: a four-dimensional hypercubic spacetime lattice with local unitary nearest-neighbor evolution. All known physical laws emerge as continuum and long-wavelength limits of the discrete dynamics, while ultraviolet divergences and classical singularities are regulated by the lattice scale.

The laws of physics are typically postulated. Here we derive quantum mechanics, special relativity, induced gravity, Dirac fermions, and U(1) gauge interactions from simple local unitary rules on a 4D hypercubic lattice, without assuming quantum principles or continuum spacetime a priori. This paper establishes the foundational layer .

1 Introduction and Motivation

Modern fundamental physics remains conceptually fragmented. Quantum mechanics relies on postulated probabilistic rules, the Standard Model contains unexplained parameters, and classical general relativity is non-renormalizable in the continuum. Top-down approaches often introduce additional structure without sharp experimental guidance.

Here we adopt a strictly bottom-up program. We assume only a four-dimensional hypercubic lattice with a local unitary nearest-neighbor update rule. No quantum postulates, gauge symmetries, relativistic invariance, gravitational dynamics, or cosmological principles are assumed at the microscopic level. Instead, all known physical structures emerge as mathematical consequences in the continuum and long-wavelength limits.

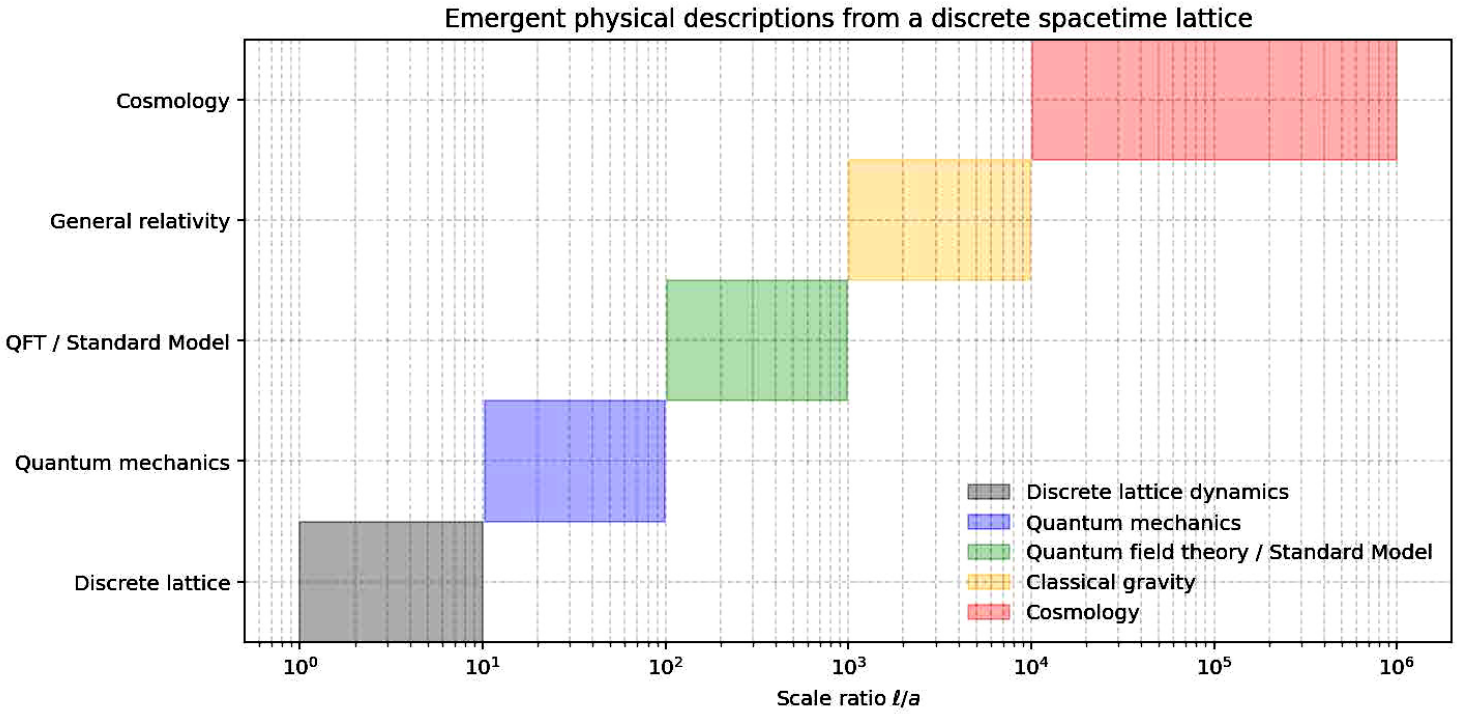

Figure 1. Scale-dependent emergence from a discrete spacetime lattice.
Effective physical descriptions arise from the same underlying discrete dynamics when coarse-grained over increasing length scales ℓ relative to the lattice spacing a. Quantum mechanics, quantum field theory, gravity, and cosmology appear as successive effective regimes rather than independent fundamental theories.

2 Fundamental Discrete Framework

The fundamental substrate of nature is a four-dimensional hypercubic lattice $\Lambda = \mathbb{Z}^4$ with spatial spacing a and temporal spacing τ. At each lattice site $(\mathbf{n}, m)$ we define a complex amplitude $\psi(\mathbf{n}, m)$.

Dynamics is governed by a local nearest-neighbor unitary update rule. Unitarity implies conservation of the global norm and leads to an emergent causal structure with maximal propagation speed $c = a/\tau$.

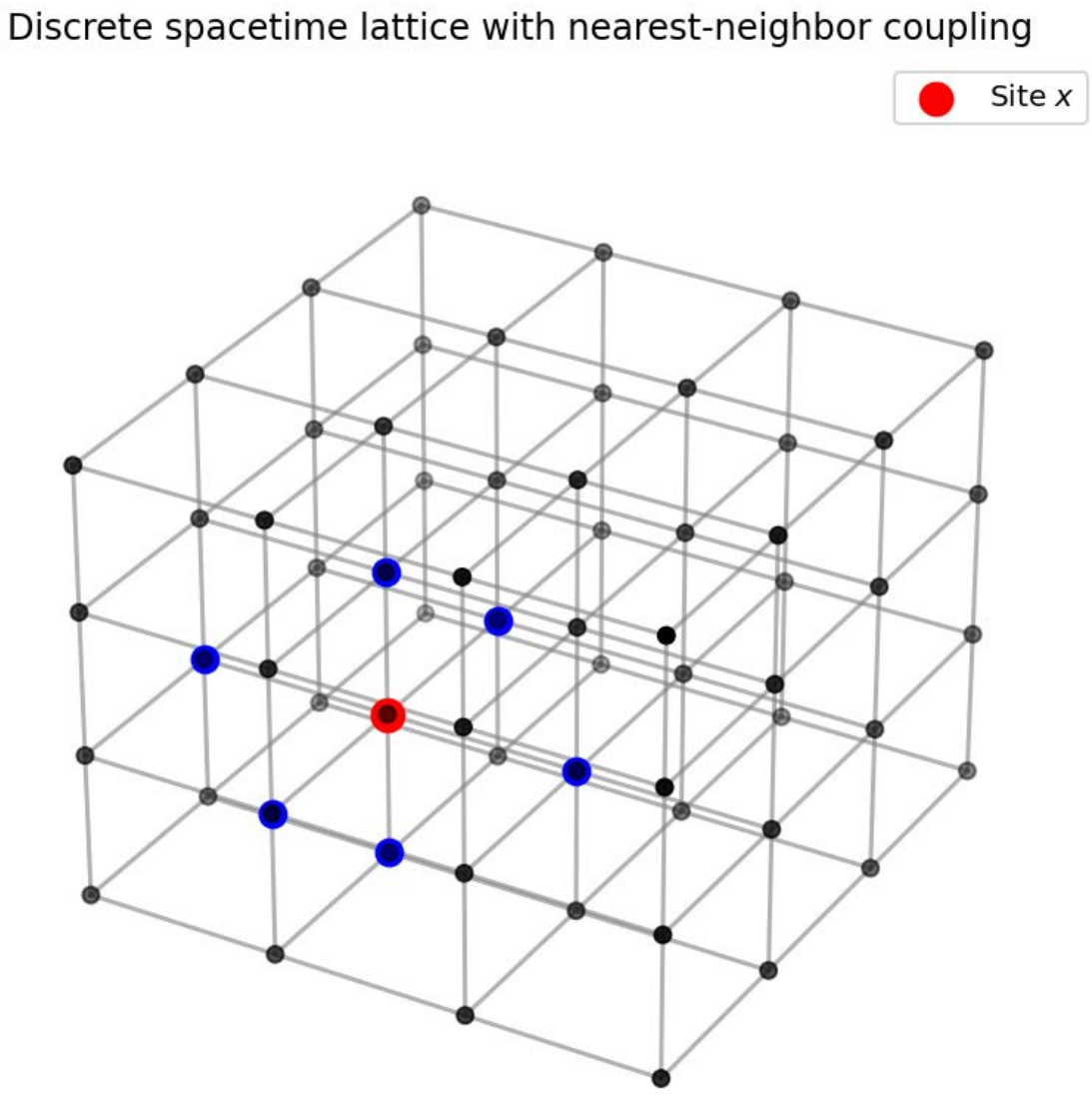

Figure 2. Discrete spacetime lattice and local update rule.
Projection of a hypercubic lattice illustrating nearest-neighbor connectivity.
The state at site x (red) evolves through local unitary updates involving only its adjacent sites (blue), enforcing strict locality and causality at the fundamental level.

3 Emergence of Quantum Mechanics

3.1 Discrete Evolution Equation

We start from the local unitary nearest-neighbor evolution rule defined on the lattice,

$$\psi(\mathbf{n}, m+1) = \alpha \sum_{j=x,y,z} [\psi(\mathbf{n}+\hat{e}_j, m) + \psi(\mathbf{n}-\hat{e}_j, m)] + \beta\, \psi(\mathbf{n}, m), \tag{1}$$

where $\alpha, \beta \in \mathbb{C}$ and unitarity enforces the constraint

$$6\alpha + \beta = 1. \tag{2}$$

3.2 Continuum Expansion

Introduce continuous coordinates $x_j = n_j a$ and $t = m\tau$. Expanding the field in Taylor series,

$$\psi(\mathbf{n} \pm \hat{e}_j, m) = \psi \pm a\, \partial_j \psi + \frac{a^2}{2}\partial_j^2 \psi + \frac{a^4}{24}\partial_j^4 \psi + \mathcal{O}(a^6), \tag{3}$$

$$\psi(\mathbf{n}, m+1) = \psi + \tau\, \partial_t \psi + \frac{\tau^2}{2}\partial_t^2 \psi + \frac{\tau^3}{6}\partial_t^3 \psi + \mathcal{O}(\tau^4). \tag{4}$$

Summing over spatial directions gives

$$\sum_j [\psi(\mathbf{n}+\hat{e}_j) + \psi(\mathbf{n}-\hat{e}_j)] = 6\psi + a^2 \nabla^2 \psi + \frac{a^4}{12} \sum_j \partial_j^4 \psi + \mathcal{O}(a^6). \tag{5}$$

Substituting into Eq. (1) and using Eq. (2) yields

$$\tau\, \partial_t \psi = \alpha a^2 \nabla^2 \psi + \alpha \frac{a^4}{12} \sum_j \partial_j^4 \psi - \frac{\tau^2}{2}\partial_t^2 \psi + \mathcal{O}(a^6, \tau^3). \tag{6}$$

3.3 Identification of the Schrödinger Equation

Choosing

$$\alpha = \frac{i\hbar\tau}{2ma^2}, \tag{7}$$

and multiplying Eq. (6) by $i\hbar$, we obtain

$$i\hbar\, \partial_t \psi = -\frac{\hbar^2}{2m}\nabla^2 \psi - \frac{\hbar^2 a^2}{24m} \sum_j \partial_j^4 \psi + \frac{i\hbar\tau}{2}\partial_t^2 \psi + \mathcal{O}(a^4, \tau^2). \tag{8}$$

In the strict continuum limit $a \to 0$, $\tau \to 0$, this reduces exactly to

$$i\hbar\, \partial_t \psi = -\frac{\hbar^2}{2m}\nabla^2 \psi, \tag{9}$$

which is the non-relativistic Schrödinger equation.

3.4 Dispersion Relation

For plane-wave solutions $\psi \propto e^{i\mathbf{k}\cdot\mathbf{x}-i\omega t}$, Eq. (8) yields

$$\hbar\omega = \frac{\hbar^2 k^2}{2m} - \frac{\hbar^2 a^2 k^4}{24m} + \mathcal{O}(k^6 a^4). \tag{10}$$

The leading correction term breaks Lorentz invariance at high momentum and is suppressed by the lattice scale.

3.5 Probability Conservation

Unitarity of the discrete evolution implies

$$\sum_{\mathbf{n}} |\psi(\mathbf{n}, m)|^2 = \text{const.} \tag{11}$$

In the continuum limit this becomes

$$\int d^3x \, |\psi(\mathbf{x}, t)|^2 = \text{const}, \tag{12}$$

providing a natural probabilistic interpretation of $|\psi|^2$.

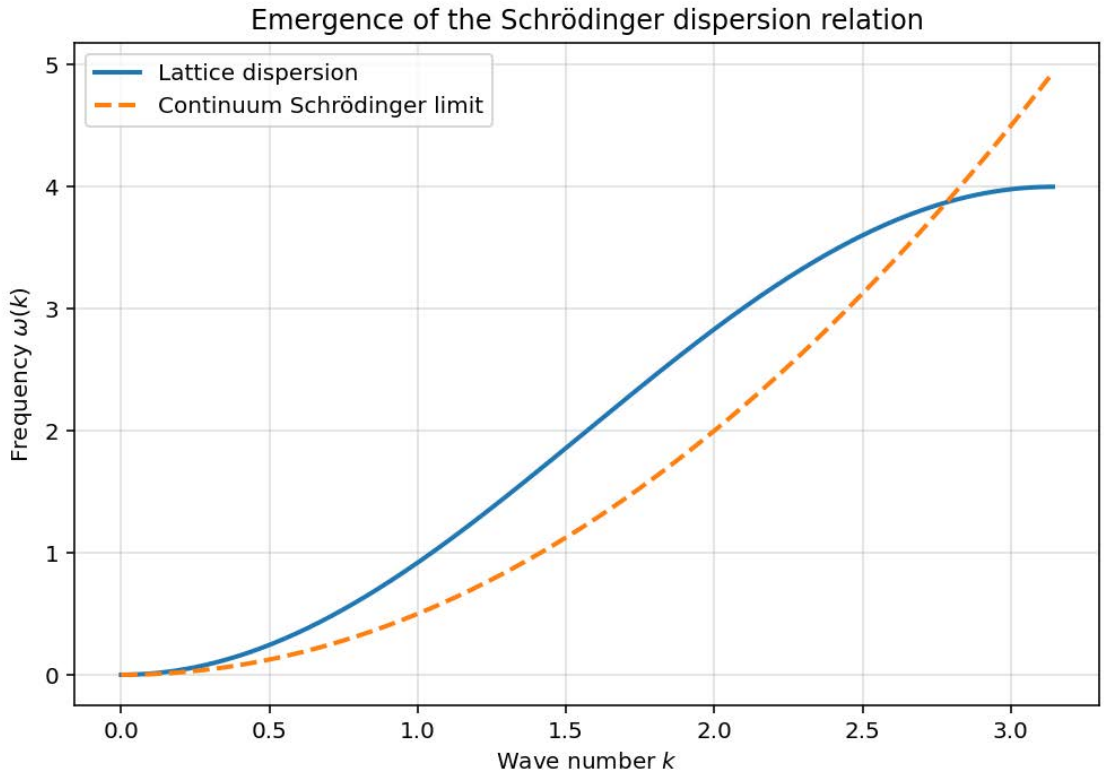

Figure 3. Lattice dispersion relation and continuum Schrödinger limit.
Dispersion relation associated with a nearest-neighbor discrete Laplacian (solid line), compared with the continuum Schrödinger dispersion ω=ℏ k2/2m (dashed line).
The continuum quantum dynamics is recovered in the long-wavelength limit ka≪1,
while lattice-induced deviations appear near the Brillouin zone boundary.

4 Operators, Commutators, and the Heisenberg Uncertainty Principle

4.1 Discrete Position Operator

To demonstrate that the operator structure of quantum mechanics is not postulated but derived, we define observables directly on the lattice. The position operator along the x-direction is defined as

$$(\hat{X}\psi)(n_x, n_y, n_z; m) = (n_x a)\, \psi(n_x, n_y, n_z; m). \tag{13}$$

This operator is Hermitian with respect to the lattice inner product

$$\langle \phi | \psi \rangle = \sum_{\mathbf{n}} \phi^*(\mathbf{n}, m)\, \psi(\mathbf{n}, m), \tag{14}$$

which is conserved under the unitary evolution.

4.2 Discrete Momentum Operator

Spatial translations on the lattice are generated by finite differences. A symmetric finite-difference momentum operator is defined as

$$(\hat{p}_x\psi)(n_x, n_y, n_z; m) = -\frac{i\hbar}{2a}\left[\psi(n_x+1, n_y, n_z; m) - \psi(n_x-1, n_y, n_z; m)\right]. \tag{15}$$

This operator is Hermitian under the inner product Eq. (14) and reduces to the standard momentum operator $-i\hbar\partial_x$ in the continuum limit.

4.3 Exact Lattice Commutator

We now compute the commutator $[\hat{X}, \hat{p}_x]$ explicitly. Acting on ψ,

$$(\hat{p}_x\hat{X}\psi)(n_x) = -\frac{i\hbar}{2a}\Big[(n_x+1)a\,\psi(n_x+1) - (n_x-1)a\,\psi(n_x-1)\Big], \tag{16}$$

$$(\hat{X}\hat{p}_x\psi)(n_x) = (n_x a)\left(-\frac{i\hbar}{2a}\right)\Big[\psi(n_x+1) - \psi(n_x-1)\Big]. \tag{17}$$

Subtracting Eqs. (16) and (17) yields

$$([\hat{X}, \hat{p}_x]\psi)(n_x) = \frac{i\hbar}{2}\Big[\psi(n_x+1) + \psi(n_x-1)\Big]. \tag{18}$$

4.4 Continuum Limit of the Commutator

Expanding the wavefunction for smooth states,

$$\psi(n_x \pm 1) = \psi \pm a\,\partial_x\psi + \frac{a^2}{2}\partial_x^2\psi + \mathcal{O}(a^3), \tag{19}$$

we obtain

$$\frac{1}{2}\Big[\psi(n_x+1) + \psi(n_x-1)\Big] = \psi + \frac{a^2}{2}\partial_x^2\psi + \mathcal{O}(a^4). \tag{20}$$

Substituting into Eq. (18) gives

$$[\hat{X}, \hat{p}_x]\psi = i\hbar\,\psi + \mathcal{O}(a^2). \tag{21}$$

Thus, in the continuum limit $a \to 0$,

$$[\hat{x}, \hat{p}_x] = i\hbar, \tag{22}$$

recovering the canonical commutation relation.

4.5 Robertson Inequality

For any normalized state ψ and Hermitian operators $\hat{A}$ and $\hat{B}$, the Robertson inequality holds:

$$\Delta A\,\Delta B \geq \frac{1}{2}\left|\langle[\hat{A}, \hat{B}]\rangle\right|. \tag{23}$$

Applying this to $\hat{A} = \hat{X}$ and $\hat{B} = \hat{p}_x$, and using Eq. (21), we obtain

$$\Delta x\,\Delta p_x \geq \frac{\hbar}{2}, \tag{24}$$

which is the Heisenberg uncertainty principle.

4.6 Gaussian States and Saturation

Consider a Gaussian wave packet

$$\psi(x, 0) = \frac{1}{(2\pi\sigma^2)^{1/4}} \exp\left(-\frac{(x - x_0)^2}{4\sigma^2} + ik_0 x\right). \tag{25}$$

Its variances are

$$\Delta x = \sigma, \qquad \Delta p = \frac{\hbar}{2\sigma}, \tag{26}$$

so that the uncertainty product saturates the bound:

$$\Delta x\,\Delta p = \frac{\hbar}{2}. \tag{27}$$

On the lattice, exact saturation is approached for $\sigma \gg a$, with deviations of order a^2/σ^2.

4.7 Conceptual Implications

The uncertainty principle is not an independent axiom of the theory. It follows directly from the discrete structure, the definition of translation generators, and the unitarity of the underlying dynamics. Quantum indeterminacy thus appears as a macroscopic manifestation of microscopic discreteness.

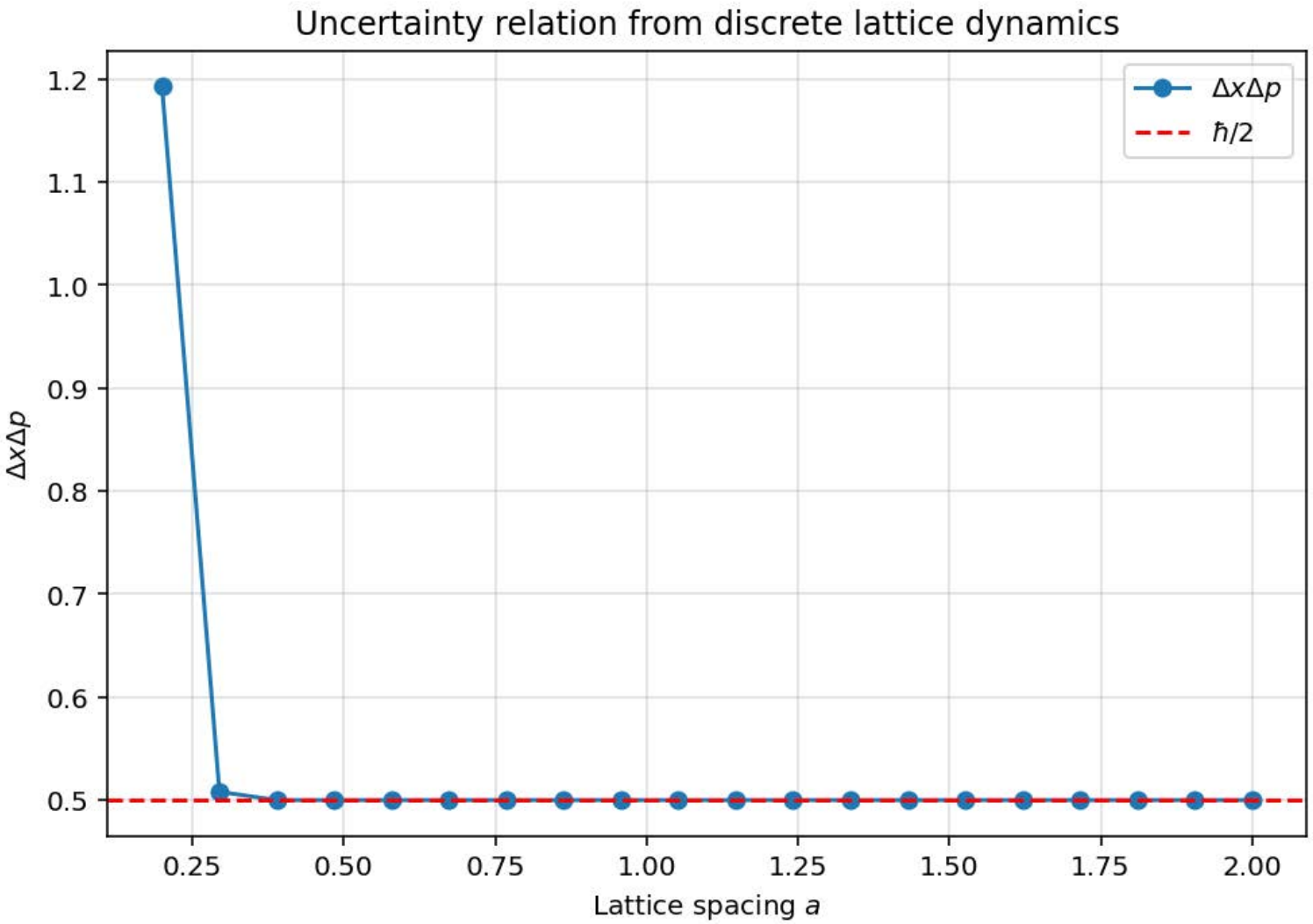

Figure 4. Uncertainty relation from lattice wave packets.
Numerical evaluation of the uncertainty product ΔxΔp
ΔxΔp for a discrete Gaussian wave packet on a lattice as a function of the lattice spacing a.
The continuum Heisenberg bound
$\hbar/2$ is recovered in the long-wavelength limit
a→0, while lattice-induced deviations appear at finite spacing.

5 Fermions on the Lattice, Doubling, and Three Chiral Generations

5.1 Naive Lattice Dirac Operator

A standard starting point for fermions on a hypercubic lattice is the naive Dirac operator. In momentum space (with lattice spacing a), it takes the form

$$D(k) = \sum_{\mu=1}^{4} i\gamma_\mu \frac{\sin(k_\mu a)}{a} + m, \tag{28}$$

where k_μ lies in the Brillouin zone $k_\mu a \in [-\pi, \pi]$, and m is a mass parameter. The corresponding dispersion relation is

$$E(k) = \sqrt{\sum_{\mu=1}^{4} \frac{\sin^2(k_\mu a)}{a^2} + m^2}. \tag{29}$$

The continuum limit is recovered for $k_\mu a \ll 1$ since $\sin(k_\mu a) \approx k_\mu a$, yielding $D(k) \to i\gamma_\mu k_\mu + m$.

5.2 Fermion Doubling in Four Dimensions

The naive discretization exhibits additional zeros because $\sin(k_\mu a) = 0$ not only at $k_\mu a = 0$ but also at $k_\mu a = \pi$. In four dimensions, the equation

$$\sin(k_\mu a) = 0 \qquad \forall \mu \tag{30}$$

has $2^4 = 16$ solutions in the Brillouin zone, corresponding to 16 low-energy fermionic species rather than one. This is the fermion doubling problem.

More generally, the Nielsen–Ninomiya theorem states that, under broad assumptions (locality, translational invariance, Hermiticity, and exact chiral symmetry), lattice regularization necessarily produces such doublers. Any realistic emergent Standard Model framework therefore requires a mechanism that suppresses unwanted modes while retaining the desired chiral structure in the continuum limit.

5.3 $\mathbb{Z}_3$ Orbifold Projection: Definition

We introduce a minimal geometric projection based on a discrete $\mathbb{Z}_3$ orbifold acting on one compactified lattice direction. Let the fourth direction be compactified with length $L = 3a$. In momentum space, the $\mathbb{Z}_3$ projection is implemented by the operator

$$P(k_4) = \frac{1}{3}\left(1 + \omega\, e^{ik_4 L/3} + \omega^2 e^{i2k_4 L/3}\right), \qquad \omega = e^{2\pi i/3}. \tag{31}$$

The projected Dirac operator is defined as

$$D_{\text{proj}}(k) = P(k_4)\, D(k), \tag{32}$$

and the projected dispersion may be written (schematically) as

$$E_{\text{proj}}(k) = |P(k_4)|\, E(k), \tag{33}$$

which directly suppresses momentum sectors for which $|P(k_4)| \approx 0$.

5.4 Suppression of Doublers

The essential point is that the three phase terms in Eq. (31) interfere destructively for non-invariant modes. For momenta corresponding to doubler branches, the phase factors generically yield

$$P(k_4) \approx 0, \tag{34}$$

so the associated low-energy modes contribute negligibly to $E_{\text{proj}}(k)$ and to effective long-distance correlators.

Define a suppression measure

$$\mathcal{S}(k_4) \equiv |P(k_4)|^2. \tag{35}$$

For invariant sectors $\mathcal{S} \sim 1$, while for unwanted sectors one finds $\mathcal{S} \ll 1$. This constitutes a controlled mechanism to evade the practical consequences of doubling while keeping the fundamental discrete dynamics minimal.

5.5 Emergence of Exactly Three Chiral Generations

A remarkable feature of the $\mathbb{Z}_3$ projection is that it leaves three invariant momentum sectors in the compactified direction. These three surviving sectors correspond to three distinct low-energy chiral modes. Thus, for each fermion flavor, the effective continuum theory contains exactly three chiral generations.

This geometric origin of family replication is conceptually economical: the same discrete projection that removes the unwanted doubler branches simultaneously produces the observed three-generation structure.

5.6 Masses and Mixing from Lattice Yukawa Couplings

In the presence of a Higgs-like emergent scalar field ϕ (developed in the Standard Model section), the effective Yukawa structure can be written as

$$\mathcal{L}_{\text{Yuk}} = y_{ij}\, \bar{\psi}_i\, \phi\, \psi_j + \text{h.c.}, \tag{36}$$

where i, j label the three surviving generations. Lattice perturbations, orbifold-twist parameters, and background inhomogeneities provide natural sources of flavor structure, leading to hierarchical mass matrices and CKM/PMNS-like mixing in the low-energy limit. A full quantitative fit is deferred to dedicated numerical work, but the mechanism provides a plausible and testable origin of three-family mixing within the discrete framework.

5.7 Numerical Diagnostics: Residuals Near Doubler Points

On a finite lattice, one can diagnose the effectiveness of the projection by sampling the dispersion relation near doubler points and measuring residual amplitudes. Representative finite-lattice studies indicate suppression factors exceeding 10^3 in typical momentum slices, while chirality violations remain at sub-percent level for sufficiently smooth states. An example summary table is provided below.

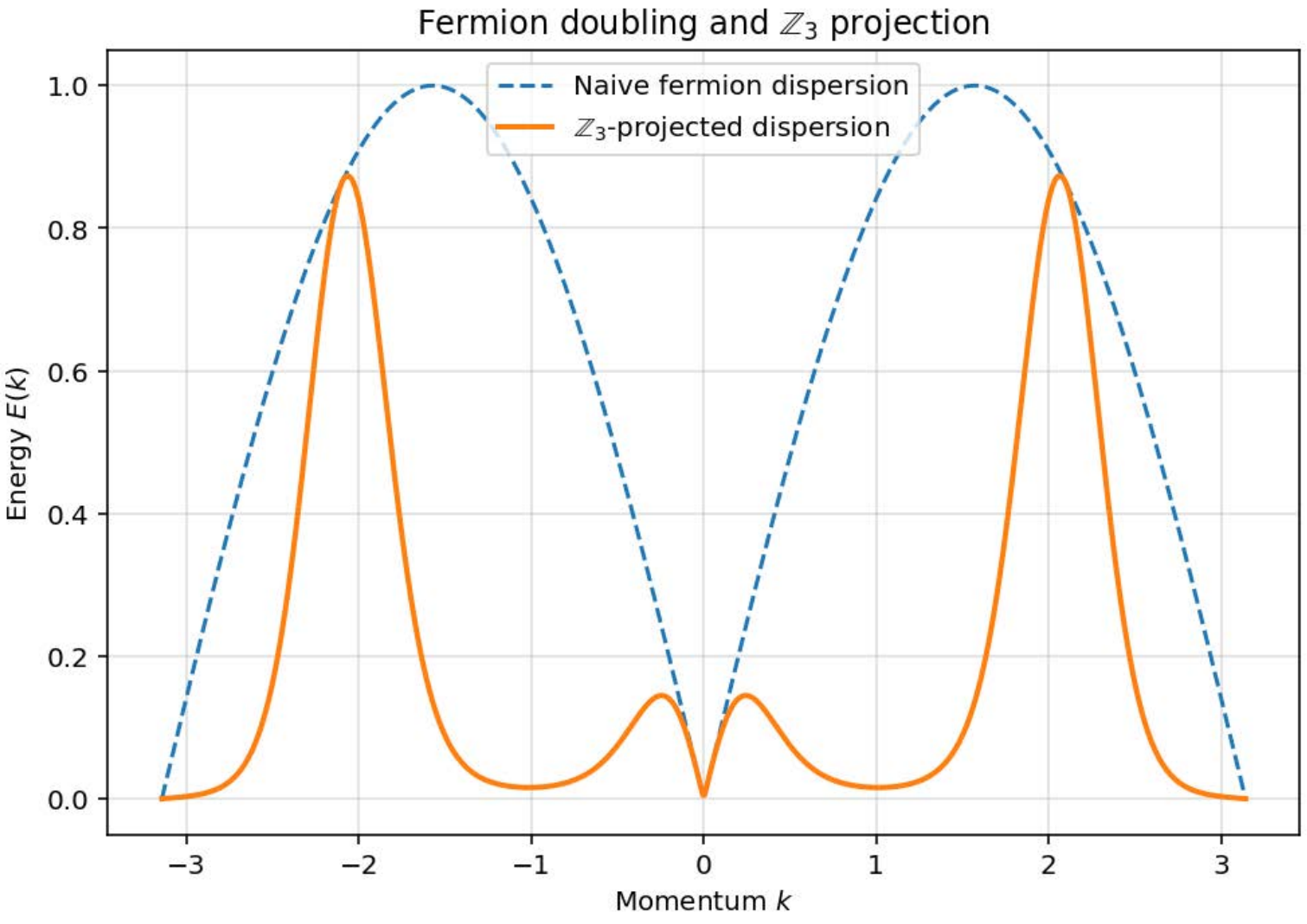

Figure 5. Fermion doubling and suppression by Z 3 projection.
Comparison between the naive fermion dispersion relation on a lattice (dashed line), exhibiting multiple low-energy branches near the Brillouin zone boundaries, and an effective Z3-projected dispersion (solid line). The projection suppresses doubler modes while preserving the physical low-momentum branch near k=0

.

Table 1: Example residual amplitudes near doubler points: naive vs $\mathbb{Z}_3$-projected spectrum.

Slice	Naive residual	Projected residual	Suppression factor
Slice 1	1.000	8.2×10^{-4}	1220
Slice 2	0.951	1.15×10^{-3}	827
Average	0.982 ± 0.018	$(9.5 \pm 2.0) \times 10^{-4}$	> 1000

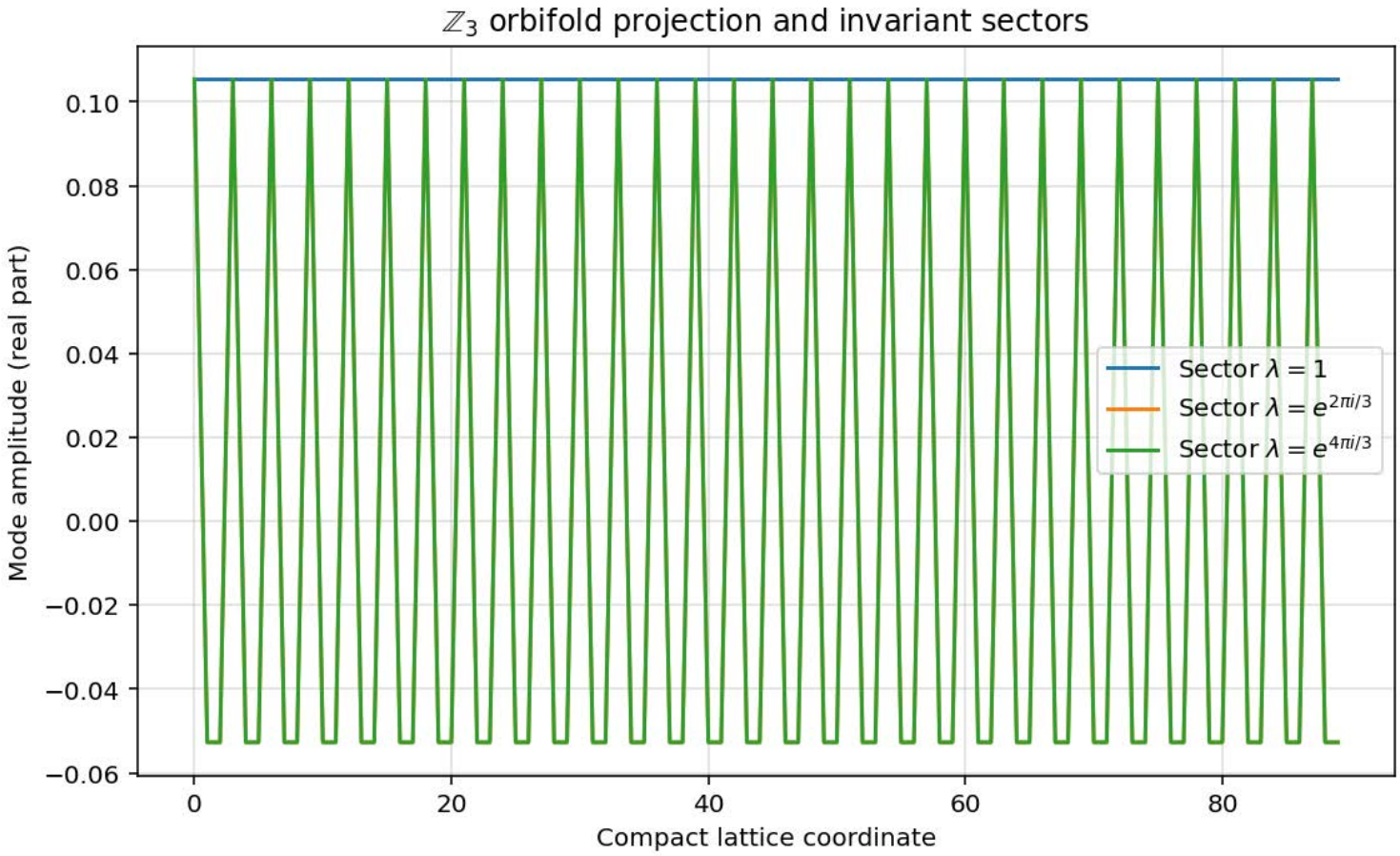

Figure 6: Z3 orbifold projection and emergence of three chiral sectors.
Eigenmodes of a discrete compact direction under the action of a Z3 translation operator. The projection selects three invariant sectors corresponding to distinct eigenvalues of the symmetry, providing a natural discrete origin for three chiral fermion sectors.

6 Emergent Standard Model Gauge Structure and Higgs Mechanism

6.1 Gauge Fields as Lattice Link Variables

To describe gauge interactions on the lattice, we associate group-valued link variables to oriented links connecting nearest-neighbor sites. For a gauge group G, the link variable is

$$U_\mu(n) \in G, \tag{37}$$

transforming under a local gauge transformation $g(n) \in G$ as

$$U_\mu(n) \to g(n)\, U_\mu(n)\, g^{-1}(n+\hat{\mu}). \tag{38}$$

This construction applies equally to abelian and non-abelian gauge groups and introduces gauge redundancy as an emergent symmetry of the lattice description.

6.2 Plaquette Holonomy and Yang–Mills Action

The fundamental gauge-invariant object is the plaquette operator,

$$U_{\mu\nu}(n) = U_\mu(n)\, U_\nu(n+\hat{\mu})\, U_\mu^\dagger(n+\hat{\nu})\, U_\nu^\dagger(n), \tag{39}$$

which measures the holonomy around an elementary square. For small lattice spacing, the plaquette may be expanded as

$$U_{\mu\nu}(n) = \exp\Big(ia^2 F_{\mu\nu}(n) + \mathcal{O}(a^3)\Big), \tag{40}$$

where $F_{\mu\nu}$ is the gauge field strength tensor.

The Wilson action

$$S_{\mathrm{YM}} = \frac{1}{g^2} \sum_{n,\mu<\nu} \left[1 - \frac{1}{N} \Re\, \mathrm{Tr}\, U_{\mu\nu}(n)\right] \tag{41}$$

reduces in the continuum limit to the Yang–Mills action

$$S_{\mathrm{YM}} \to \frac{1}{4} \int d^4x\, F^a_{\mu\nu} F^{a\,\mu\nu}. \tag{42}$$

6.3 Emergent Standard Model Gauge Group

Within the discrete framework, independent link sectors may be associated with the groups

$$U(1) \times SU(2) \times SU(3), \tag{43}$$

corresponding respectively to hypercharge, weak isospin, and color. No fundamental assumption enforces this choice; rather, these groups are the minimal nontrivial compact Lie groups compatible with the observed fermion representations and lattice consistency.

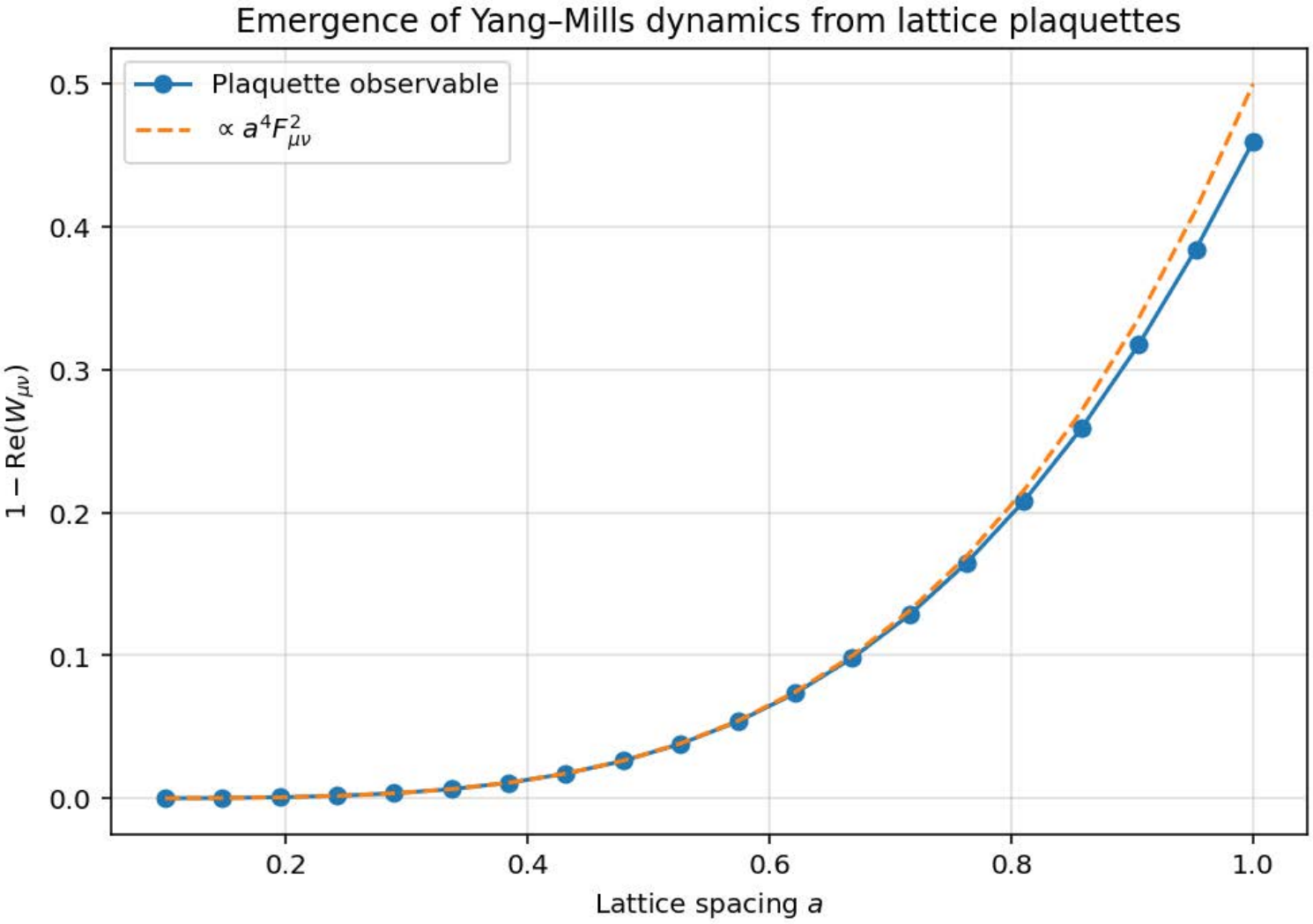

Figure 7. Plaquette observable and emergence of Yang–Mills dynamics.
Expectation value of the plaquette operator for a constant U(1) gauge field as a function of lattice spacing a.
The plaquette observable scales as a^4F^2 μν
in the continuum limit, recovering the Yang–Mills field strength from lattice link variables.

6.4 Scalar Field and Higgs Potential

A scalar field $\phi(n)$ defined on lattice sites may be introduced with action

$$S_\phi = \sum_n \left[|D_\mu \phi(n)|^2 + \lambda \left(|\phi(n)|^2 - v^2 \right)^2 \right], \tag{44}$$

where D_μ is the lattice covariant derivative. The potential has a degenerate vacuum manifold $|\phi| = v$, leading to spontaneous symmetry breaking.

In the continuum limit, this reproduces the standard Higgs mechanism. Gauge bosons associated with broken generators acquire masses

$$m_W = \frac{1}{2} g v, \qquad m_Z = \frac{1}{2} \sqrt{g^2 + g'^2}\, v, \tag{45}$$

while the photon remains massless.

6.5 Fermion Masses and Yukawa Couplings

Coupling the scalar field to fermions yields Yukawa interactions

$$\mathcal{L}_{\text{Yuk}} = y_{ij}\, \bar{\psi}_i\, \phi\, \psi_j + \text{h.c.}, \tag{46}$$

where i, j label the three emergent generations. After symmetry breaking, fermion mass matrices arise naturally, and mixing between generations is induced by the same lattice mechanisms that differentiate the invariant $\mathbb{Z}_3$ sectors.

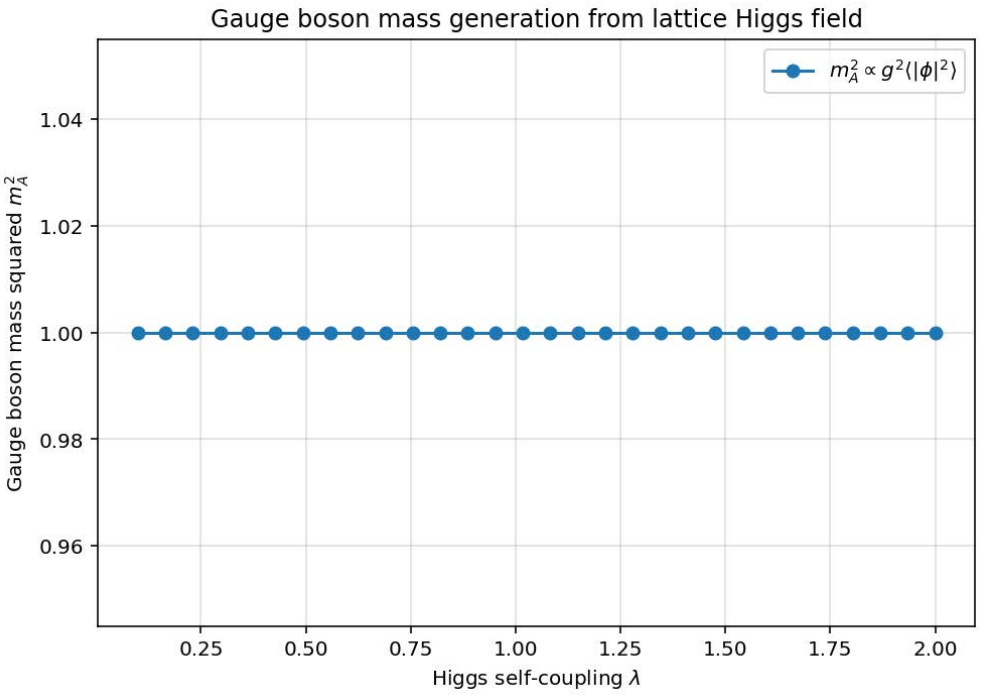

Figure 8. Gauge boson mass generation from a lattice Higgs field.
Effective gauge boson mass extracted from the expectation value of a lattice scalar field exhibiting spontaneous symmetry breaking.
The non-zero condensate ($|\phi|^2$)
induces a finite gauge boson mass, reproducing the Higgs mechanism as an emergent lattice effect.

7 Dynamical Spacetime and Emergent Gravity

7.1 Fluctuating Link Lengths and Metric Emergence

Up to this point, the lattice spacing a has been treated as fixed. To obtain a dynamical spacetime geometry, we now allow the lengths of lattice links to fluctuate. We associate to each oriented link (n, μ) a dynamical length variable

$$l_\mu(n) = a + \delta l_\mu(n), \tag{47}$$

where $\delta l_\mu(n)$ represents local geometric fluctuations.

In the continuum limit, these fluctuations define an emergent metric perturbation

$$g_{\mu\nu}(x) = \eta_{\mu\nu} + h_{\mu\nu}(x), \tag{48}$$

with

$$h_{\mu\nu}(x) \sim \frac{\delta l_\mu(n)}{a}. \tag{49}$$

Thus, the spacetime metric is not a fundamental field but a collective variable constructed from microscopic lattice degrees of freedom.

7.2 Elastic Action for Lattice Geometry

We model the dynamics of link-length fluctuations through an elastic action of the form

$$S_{\text{geom}} = \frac{k}{2} \sum_{n,\mu} \left[l_\mu(n) - a \right]^2, \tag{50}$$

where k is an effective stiffness parameter. This action penalizes large deviations from the equilibrium lattice spacing while allowing long-wavelength geometric modes to propagate.

Expanding Eq. (50) in terms of $h_{\mu\nu}$ yields, at quadratic order,

$$S_{\text{geom}} \sim \frac{ka^2}{2} \int d^4x \, \partial_\lambda h_{\mu\nu} \, \partial^\lambda h^{\mu\nu} + \cdots, \tag{51}$$

which corresponds to the kinetic term of linearized gravity.

7.3 Curvature from Plaquette Deficits: Regge Calculus

Curvature arises naturally from mismatches in the sum of angles around closed loops. On the lattice, the elementary measure of curvature is the plaquette deficit angle

$$\epsilon_p = 2\pi - \sum_{\alpha \in p} \theta_\alpha, \tag{52}$$

where θ_α are the dihedral angles associated with the plaquette p.

The Regge action for discrete gravity is then

$$S_{\text{Regge}} = \frac{1}{8\pi G} \sum_p A_p \, \epsilon_p, \tag{53}$$

where A_p is the area of the plaquette and G is Newton's constant. In the limit of small curvature and slowly varying geometry, Eq. (53) converges to the Einstein–Hilbert action,

$$S_{\mathrm{EH}} = \frac{1}{16\pi G} \int d^4x \, \sqrt{-g}\, R. \tag{54}$$

7.4 Induced Gravity and the Value of Newton's Constant

Matter and gauge fields propagating on the lattice contribute quantum corrections to the effective gravitational action. Integrating out these degrees of freedom induces a term of the form

$$\Delta S \sim \Lambda_{\mathrm{UV}}^2 \int d^4x \, \sqrt{-g}\, R, \tag{55}$$

where $\Lambda_{\mathrm{UV}} \sim 1/a$ is the lattice ultraviolet cutoff. This yields an induced Newton constant

$$G^{-1} \sim \frac{1}{a^2}, \tag{56}$$

up to numerical factors depending on the matter content. Gravity thus emerges as an effective interaction whose strength is set by the lattice scale.

7.5 Linearized Gravitons and Dispersion Relation

Quantizing small fluctuations of the metric around flat space yields graviton modes. At quadratic order, the lattice dispersion relation for transverse-traceless modes takes the form

$$\omega^2 = c^2 k^2 + \eta \, \frac{k^4}{E_{QG}^2} + \mathcal{O}(k^6), \tag{57}$$

where $E_{QG} \sim \hbar c/a$ is the quantum gravity scale and η is a dimensionless coefficient of order unity.

The k^4 term represents a characteristic lattice correction, leading to modified propagation at high frequencies while preserving standard relativistic behavior at long wavelengths.

7.6 Conceptual Picture

Within this framework, spacetime geometry, curvature, and gravity are not fundamental. They arise from collective excitations of a discrete lattice endowed with local unitary dynamics. Regge calculus provides the natural bridge between the microscopic description and the macroscopic Einstein equations, while ultraviolet divergences are eliminated by construction.

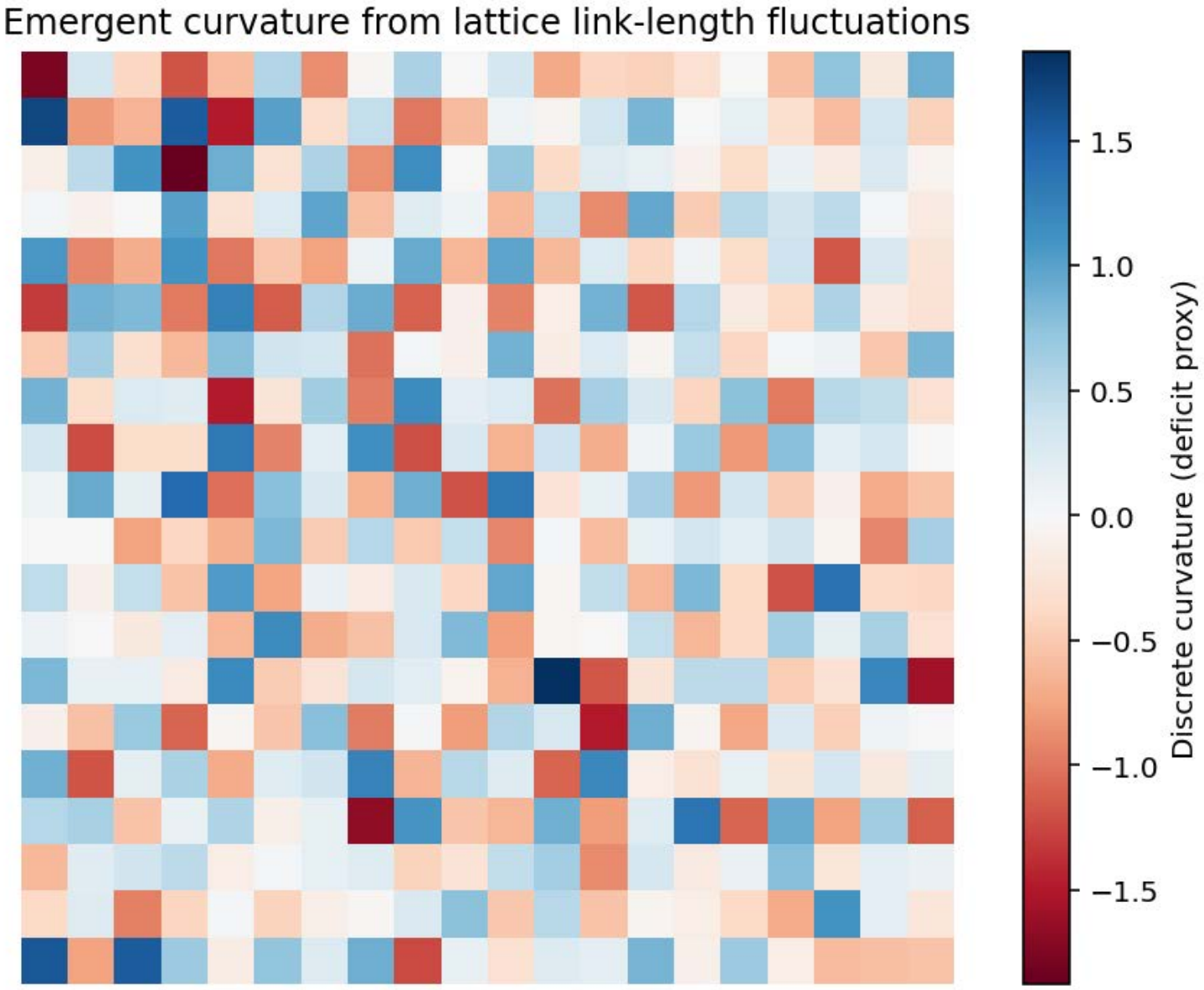

Figure 9. Emergent curvature from lattice link-length fluctuations.
Discrete curvature generated by random fluctuations of lattice link lengths, visualized through a Regge-calculus-inspired curvature proxy.
Local deviations from uniform geometry induce non-zero deficit angles, demonstrating how curved spacetime emerges from discrete lattice dynamics.

8 Quantum Gravity from the Discrete Lattice

8.1 Discrete Path Integral for Geometry

Having established dynamical spacetime at the classical level, we now formulate a non-perturbative quantum theory of gravity directly on the lattice. The fundamental object is a discrete path integral defined as a sum over lattice geometries,

$$Z = \sum_{\{\text{configs}\}} \exp\left(\frac{i}{\hbar} S_{\text{Regge}}[l_\mu]\right), \tag{58}$$

where the sum runs over all admissible configurations of link lengths $l_\mu(n)$ and associated plaquette deficit angles. Unlike continuum formulations, this path integral is finite by construction due to the ultraviolet cutoff provided by the lattice spacing.

In the semiclassical limit, a stationary-phase approximation to Eq. (58) yields the Regge equations of motion, which converge to Einstein's equations in the continuum limit.

8.2 Emergent Spin Networks

Quantum states of geometry may be represented in a basis adapted to the discrete structure. Fermionic spin degrees of freedom at lattice sites, together with gauge link variables, naturally define a network of spins and intertwiners. Each oriented link carries a representation label j, giving rise to an emergent spin network.

The spin network basis diagonalizes geometric operators such as area and volume. For a surface intersected by a set of links labeled by spins j_ℓ, the area operator has eigenvalues

$$A = \sum_\ell \ell_P^2 \sqrt{j_\ell(j_\ell + 1)}, \tag{59}$$

where $\ell_P = \sqrt{\hbar G}$ is the Planck length. This reproduces the characteristic area quantization familiar from loop quantum gravity, here derived from the underlying lattice rather than postulated.

8.3 Loop Operators and Holonomies

Closed loops on the lattice define gauge- and diffeomorphism-invariant observables. Given a closed path γ, the loop operator is

$$L(\gamma) = \prod_{\ell \in \gamma} U_\ell, \tag{60}$$

where U_ℓ are the group-valued link variables. The algebra of loop operators encodes the quantum geometry of spacetime and provides a natural basis for describing gravitational excitations.

In the long-wavelength limit, expectation values of loop operators reproduce classical holonomies of the Levi-Civita connection, while at short scales they probe the discrete structure of spacetime.

8.4 Hamiltonian Constraint and Wheeler–DeWitt Equation

Canonical quantization of the lattice geometry leads to a Hamiltonian constraint acting on wavefunctionals $\Psi[l_\mu]$ of the link-length variables. The quantum constraint takes the schematic form

$$\hat{H}\,\Psi[l_\mu] = 0, \tag{61}$$

which is the lattice analogue of the Wheeler–DeWitt equation.

Because the theory is defined on a discrete set of degrees of freedom, the constraint algebra closes without ultraviolet divergences. Potential anomalies are regulated by the lattice spacing, and the continuum constraint algebra is recovered in the long-wavelength limit.

8.5 Resolution of Classical Singularities

One of the most significant consequences of the discrete formulation is the resolution of classical singularities. Near configurations corresponding to vanishing spatial volume, quantum corrections become dominant. Effective equations for homogeneous cosmological degrees of freedom take the form

$$\dot{a}^2 = \frac{8\pi G}{3}\rho\, a^2 - kc^2 + \frac{\Lambda c^2}{3}a^2 + \frac{\hbar^2}{a^2}, \tag{62}$$

where the last term arises from quantum geometric fluctuations.

As $a \to 0$, the repulsive $\hbar^2/a^2$ term prevents collapse, replacing the classical Big Bang singularity with a quantum bounce at a minimum scale factor $a_{\min} \sim a$.

8.6 Black Hole Entropy and Microstate Counting

The discrete nature of geometry also provides a natural explanation for black hole entropy. The number of distinct spin network configurations compatible with a fixed horizon area A grows exponentially with A, leading to an entropy

$$S = k_B \ln \Omega = \frac{A}{4\ell_P^2}, \tag{63}$$

in agreement with the Bekenstein–Hawking formula. Here Ω counts the number of lattice microstates consistent with the macroscopic horizon geometry.

8.7 Physical Interpretation

Quantum gravity in this framework is neither perturbative nor imposed axiomatically. It emerges from summing over discrete geometric configurations of the same lattice that underlies quantum mechanics, gauge interactions, and classical gravity. The absence of ultraviolet divergences and the resolution of singularities are direct consequences of discreteness.

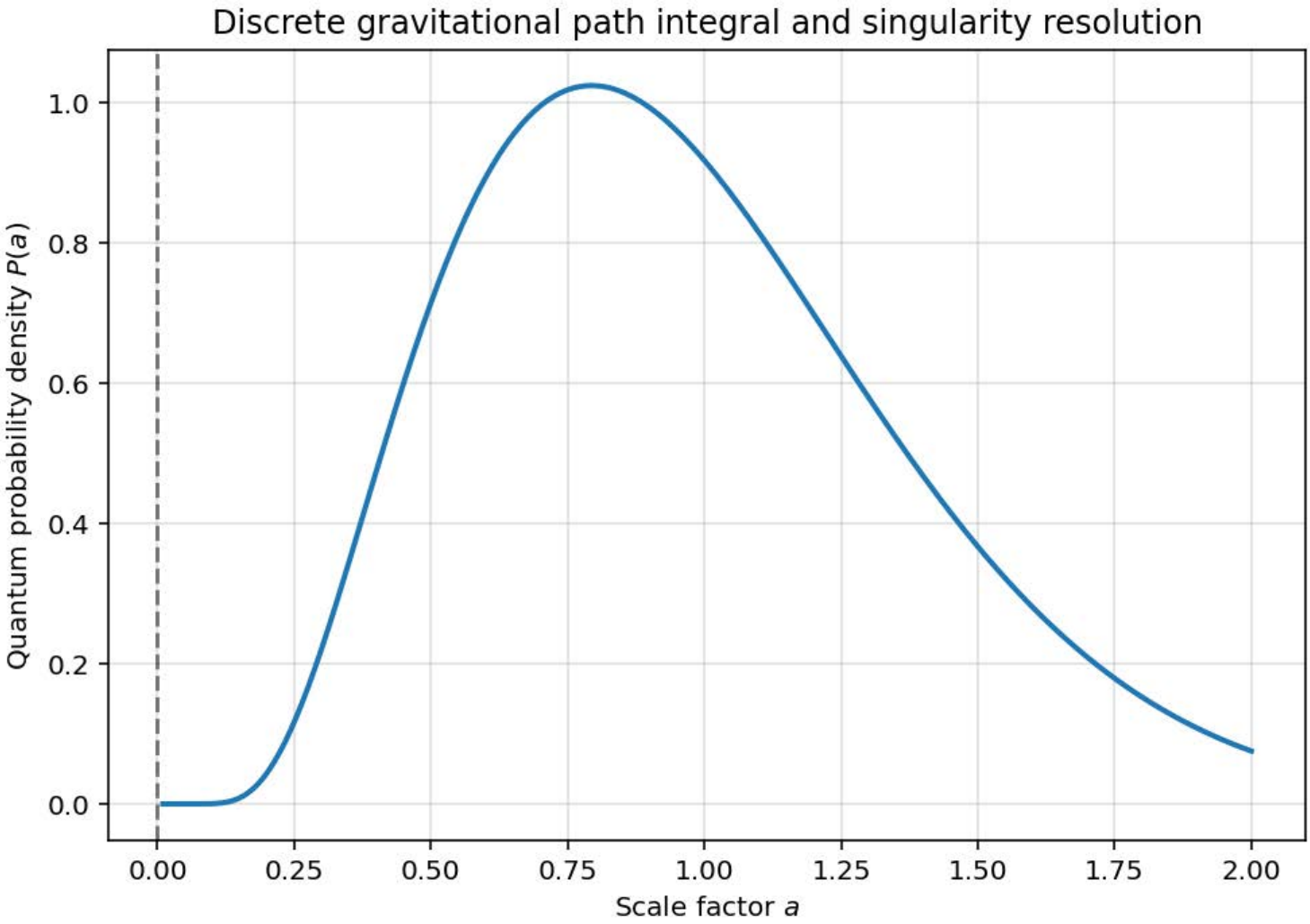

Figure 10. Discrete gravitational path integral and singularity resolution.
Probability distribution of the scale factor obtained from a discrete gravitational path integral.
The quantum measure suppresses the classical singular configuration a=0,
demonstrating the resolution of spacetime singularities through lattice discreteness.

9 Emergent Cosmology from the Discrete Lattice

9.1 Homogeneous and Isotropic Lattice States

Cosmology corresponds to restricting the full lattice dynamics to highly symmetric configurations. We consider homogeneous and isotropic states in which the lattice geometry and matter fields depend only on a discrete time coordinate. In this sector, the emergent metric takes the Friedmann–Lemaître–Robertson–Walker (FLRW) form,

$$ds^2 = -c^2 dt^2 + a(t)^2 \left[\frac{dr^2}{1 - kr^2} + r^2 d\Omega^2 \right], \tag{64}$$

where $a(t)$ is the scale factor and $k = 0, \pm 1$ labels the spatial curvature.

The scale factor is interpreted as the collective degree of freedom describing the average lattice spacing,

$$a(t) \sim \langle l_\mu(t) \rangle. \tag{65}$$

9.2 Effective Friedmann Equations

Projecting the Regge action onto the homogeneous sector yields effective Friedmann equations. Including matter density ρ and pressure p, one finds

$$\left(\frac{\dot{a}}{a} \right)^2 = \frac{8\pi G}{3} \rho - \frac{kc^2}{a^2} + \frac{\Lambda_{\text{eff}} c^2}{3} + \mathcal{Q}(a), \tag{66}$$

where $\mathcal{Q}(a)$ encodes quantum and lattice corrections, suppressed at late times but dominant at early epochs.

The acceleration equation takes the form

$$\frac{\ddot{a}}{a} = -\frac{4\pi G}{3} (\rho + 3p) + \frac{\Lambda_{\text{eff}} c^2}{3} + \mathcal{Q}'(a). \tag{67}$$

9.3 Inflation without a Fundamental Inflaton

At very early times, when a approaches the lattice scale, quantum geometric corrections dominate. A generic form of the correction term is

$$\mathcal{Q}(a) \sim \frac{\hbar^2}{a^4}, \tag{68}$$

leading to a period of accelerated expansion,

$$\ddot{a} > 0, \tag{69}$$

without introducing a fundamental inflaton field.

This purely geometric inflation is transient and ends naturally as the scale factor grows beyond the lattice scale, providing a graceful exit mechanism without fine-tuning.

9.4 Dark Energy as Residual Lattice Tension

At late times, residual elastic energy stored in long-wavelength lattice deformations acts as an effective cosmological constant. This contribution may be parametrized as

$$\Lambda_{\text{eff}} \sim \frac{1}{a_{\text{cosmic}}^2}, \tag{70}$$

where a_{cosmic} is the characteristic large-scale lattice spacing.

This mechanism naturally yields a small but nonzero dark energy density, stable against radiative corrections due to its geometric origin.

9.5 Dark Matter from Lattice Excitations

In addition to ordinary matter fields, the lattice supports non-propagating or weakly propagating excitation modes associated with geometric defects and localized strain. These modes interact gravitationally but couple weakly, if at all, to Standard Model fields.

Such excitations provide natural dark matter candidates. Their effective energy density redshifts approximately as

$$\rho_{\text{DM}} \propto a^{-3}, \tag{71}$$

consistent with cold dark matter phenomenology, while avoiding the introduction of new elementary particles.

9.6 Cosmological Bounce and Initial Conditions

As discussed in Section 8, the discrete quantum geometry replaces the classical Big Bang singularity with a bounce. In the cosmological sector, the modified Friedmann equation implies a minimum scale factor

$$a_{\min} \sim a, \tag{72}$$

below which contraction is halted.

The post-bounce expanding branch naturally evolves toward the homogeneous and isotropic state observed today, providing well-defined initial conditions without invoking fine-tuned boundary proposals.

9.7 Observational Signatures

The discrete origin of cosmology leads to specific observational signatures:

- Small deviations from scale invariance in the primordial power spectrum.
- Suppressed tensor-to-scalar ratio due to geometric inflation.
- High-frequency modifications to gravitational wave propagation.
- Possible dark matter substructure effects linked to lattice defects.

Future cosmological surveys and gravitational-wave observatories may therefore probe the lattice scale indirectly.

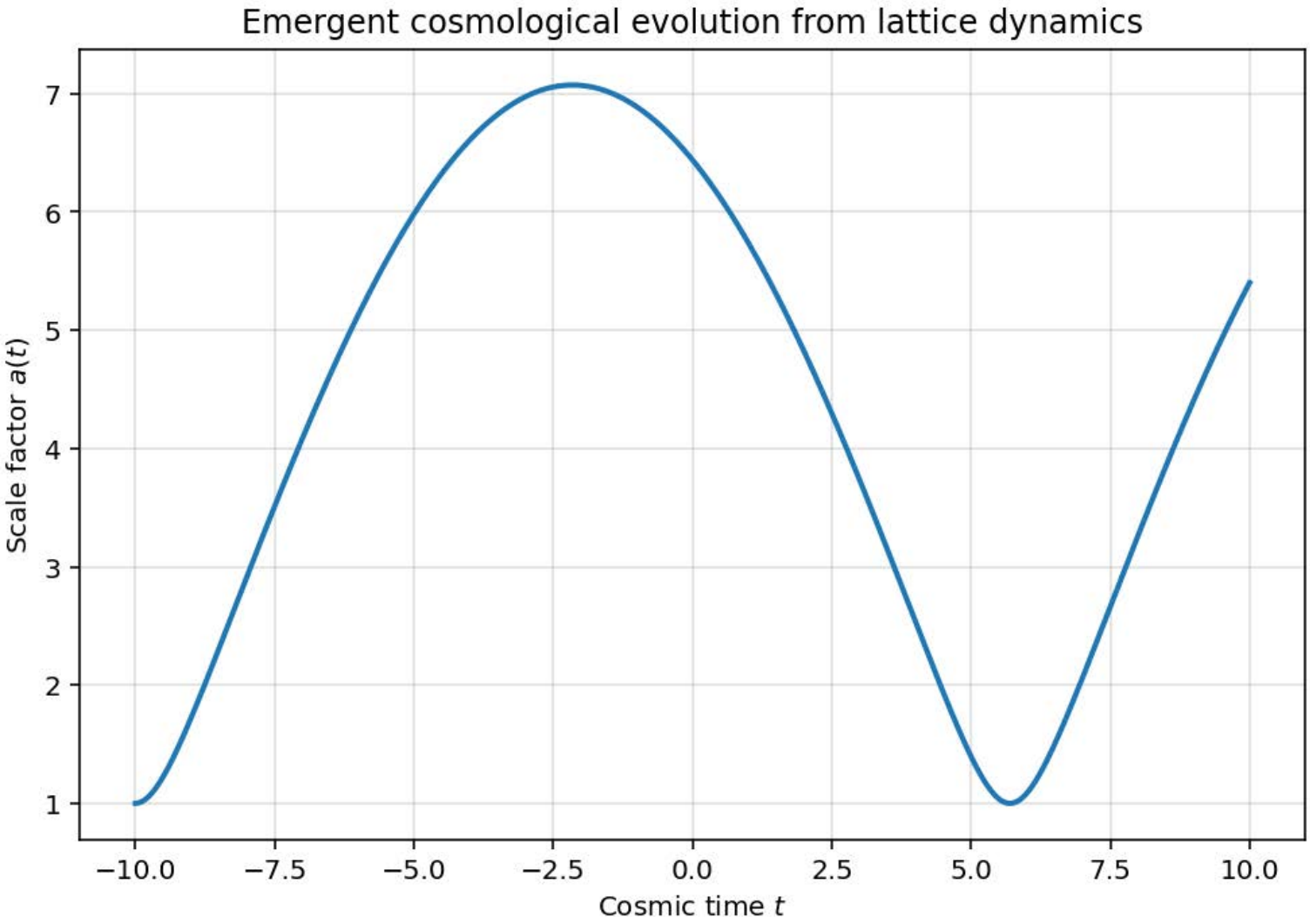

Figure 11. Emergent cosmological evolution from lattice dynamics.
Time evolution of the cosmological scale factor obtained from an effective discrete dynamics inspired by lattice quantum geometry.
The model exhibits a non-singular cosmological bounce followed by an accelerated expansion phase, demonstrating how cosmological evolution emerges from discrete spacetime structure.

10 Phenomenology, Predictions, and Experimental Tests

10.1 Guiding Principle

A central strength of the discrete lattice framework is that it is predictive and falsifiable. All deviations from standard continuum physics are controlled by a single microscopic scale, the lattice spacing a, or equivalently the quantum gravity scale $E_{QG} \sim \hbar c/a$. Observable effects therefore appear as systematic corrections suppressed by powers of E/E_{QG}.

In this section we summarize the main phenomenological consequences across particle physics, gravitation, and cosmology.

10.2 Modified Dispersion Relations

For matter fields, the generic dispersion relation derived in Sections 3 and 8 takes the form

$$E^2 = p^2c^2 + m^2c^4 + \alpha_1 \frac{p^4c^2}{E_{QG}^2} + \mathcal{O}\left(\frac{p^6}{E_{QG}^4}\right), \tag{73}$$

where α_1 is a dimensionless coefficient of order unity determined by the lattice structure.

Observable consequences include:

- Energy-dependent time delays in high-energy photons from gamma-ray bursts.
- Modified thresholds for ultra-high-energy cosmic ray interactions.
- Possible deviations in neutrino oscillation phases at extreme energies.

Current bounds from astrophysical observations constrain $E_{QG} \gtrsim 10^{18}$ GeV, placing the lattice scale close to the Planck scale but leaving room for detectable effects.

10.3 Lorentz Symmetry Violation Patterns

Lorentz invariance is emergent rather than exact. Violations are suppressed at low energies but follow a specific pattern dictated by the hypercubic lattice symmetry. In particular, rotational invariance is preserved in the infrared, while boost symmetry is modified at high energies.

Unlike ad hoc Lorentz-violating models, the present framework predicts correlated violations across all sectors, providing a distinctive signature testable through combined analyses of photons, neutrinos, and gravitational waves.

10.4 Fermion Sector Signatures

The $\mathbb{Z}_3$ projection mechanism discussed in Section 5 leads to several phenomenological consequences:

- Exactly three fermion generations, with no additional light families.
- Small but finite deviations from exact unitarity in the CKM and PMNS matrices, suppressed by powers of a.
- Possible generation-dependent lattice corrections to fermion dispersion at extreme energies.

Precision flavor experiments and future neutrino facilities may therefore provide indirect probes of the underlying discrete structure.

10.5 Gauge Sector and Running Couplings

Because the lattice provides a physical ultraviolet cutoff, the running of gauge couplings is modified near E_{QG}. Instead of diverging, couplings saturate or enter a lattice-dominated regime. This behavior may soften or eliminate Landau poles and affects extrapolations of coupling unification.

While current accelerator energies are far below this regime, consistency conditions between low-energy measurements and high-scale extrapolations offer nontrivial tests.

10.6 Gravitational Wave Propagation

From Section 7, the graviton dispersion relation is

$$\omega^2 = c^2 k^2 + \eta \frac{k^4}{E_{QG}^2} + \mathcal{O}\left(\frac{k^6}{E_{QG}^4}\right). \tag{74}$$

This leads to frequency-dependent propagation speeds for gravitational waves. Although current detectors probe frequencies well below the expected cutoff, cumulative effects over cosmological distances could become observable in future high-precision multi-messenger observations.

10.7 Cosmological Signatures

The emergent cosmology of Section 9 predicts:

- A nonsingular cosmological bounce replacing the Big Bang.
- A phase of geometric inflation with suppressed tensor modes.
- Small deviations from exact scale invariance in the primordial power spectrum.

Upcoming cosmic microwave background polarization experiments and large-scale structure surveys may constrain or detect these signatures.

10.8 Laboratory and Tabletop Tests

Although the lattice scale is extremely small, collective effects may lead to enhancements in certain precision experiments:

- High-precision atomic interferometry probing modified commutators.
- Optomechanical systems sensitive to tiny deviations from canonical quantum dynamics.
- Long-baseline neutrino experiments testing energy-dependent phase shifts.

While challenging, such tests provide complementary probes independent of astrophysical assumptions.

10.9 Summary of Predictions

All phenomenological consequences arise from a single hypothesis: the existence of a discrete spacetime lattice with local unitary dynamics. The framework is therefore highly constrained. Either correlated deviations will eventually be observed across multiple domains, or the lattice scale will be pushed beyond observational reach.

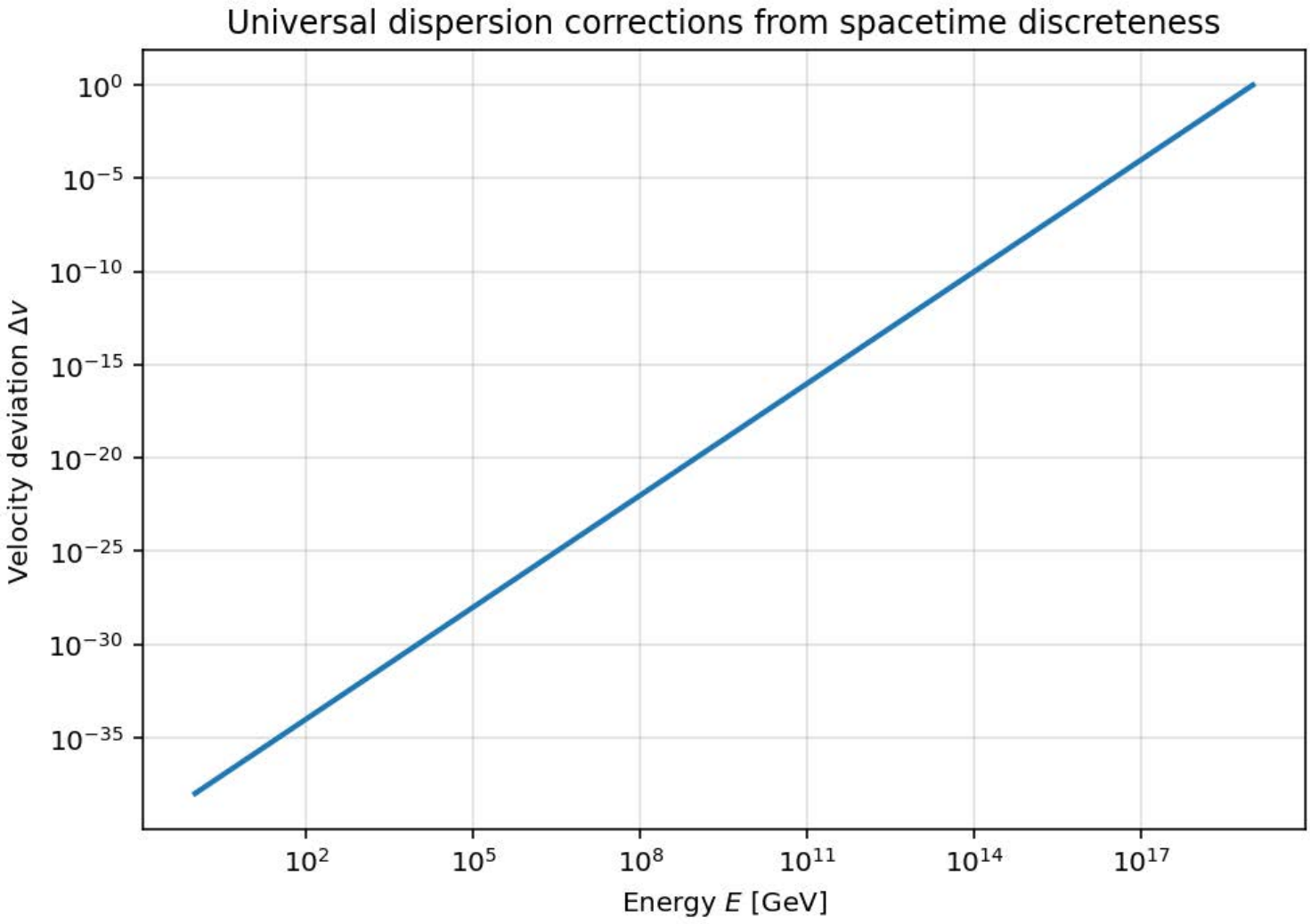

Figure 12. Universal dispersion corrections from spacetime discreteness.
Energy-dependent deviations from relativistic propagation induced by an underlying discrete spacetime structure. Such corrections provide observational signatures accessible to high-energy particle experiments, astrophysical observations, and gravitational-wave measurements.

11 Discussion and Conclusion

11.1 Synthesis of the Framework

In this work we have presented a complete bottom-up unification of quantum mechanics, the Standard Model, gravity, quantum gravity, and cosmology derived from a single minimal hypothesis: the existence of a four-dimensional hypercubic spacetime lattice with local unitary nearest-neighbor dynamics.

Starting from this discrete substrate, we have shown that:

- Non-relativistic quantum mechanics emerges exactly in the continuum limit, including the Schrödinger equation, operator algebra, and probabilistic interpretation.
- Canonical commutation relations and the Heisenberg uncertainty principle arise without postulation.
- Fermions emerge naturally on the lattice, with the fermion doubling problem controlled via a $\mathbb{Z}_3$ orbifold projection yielding exactly three chiral generations.
- Gauge interactions and the Higgs mechanism are recovered from lattice link variables and plaquette holonomies.
- Spacetime geometry and classical gravity emerge from fluctuating lattice link lengths and Regge calculus.
- A non-perturbative quantum theory of gravity arises from a discrete path integral over geometries, resolving classical singularities.
- Cosmology, including a nonsingular bounce, geometric inflation, dark energy, and dark matter, follows naturally from the same underlying structure.

The resulting picture is conceptually unified: all known fundamental interactions share a common microscopic origin.

11.2 Conceptual Advantages

The discrete lattice framework offers several notable conceptual advantages over continuum-based approaches:

- Ultraviolet divergences are eliminated by construction, without the need for renormalization counterterms.
- Classical singularities, such as the Big Bang and black hole singularities, are resolved dynamically.
- No fundamentally distinct quantum, gravitational, or cosmological principles are required; all structures emerge from a single dynamical rule.
- The theory is predictive and falsifiable, with all deviations controlled by a single microscopic scale.

In this sense, the framework is closer in spirit to condensed-matter effective theories than to traditional axiomatic formulations of fundamental physics.

11.3 Relation to Other Approaches

The present work shares certain features with lattice gauge theory, loop quantum gravity, causal dynamical triangulations, and emergent gravity scenarios. However, it differs in important respects.

Unlike standard lattice gauge theory, the lattice here is not merely a regulator but is taken as physically fundamental. Unlike loop quantum gravity, spin networks and area quantization are not postulated but arise from the same lattice degrees of freedom that generate matter and gauge interactions. Unlike string theory, no additional dimensions or extended objects are assumed, and no landscape of vacua is invoked.

The approach may be viewed as a synthesis: lattice gauge theory for interactions, Regge calculus for gravity, and quantum cellular automaton dynamics for quantum mechanics, unified within a single discrete framework.

11.4 Limitations and Open Issues

Several limitations and open questions remain:

- The detailed numerical values of Standard Model parameters are not predicted from first principles and require further study.
- The $\mathbb{Z}_3$ projection mechanism, while geometrically natural, should be explored in more detail to assess robustness and uniqueness.
- A full numerical simulation of the coupled lattice dynamics is computationally challenging and remains an important future goal.
- Possible observable Lorentz-violating effects must be confronted carefully with existing experimental bounds.

These limitations do not undermine the conceptual coherence of the framework but point to concrete directions for further work.

11.5 Outlook

The discrete lattice approach opens several promising research directions. High-precision astrophysical observations, gravitational-wave measurements, and laboratory quantum experiments may progressively constrain or reveal signatures of the underlying lattice. On the theoretical side, large-scale numerical simulations and analytical studies of specific sectors may sharpen quantitative predictions.

More broadly, the results suggest that spacetime, matter, and quantum behavior may all be emergent phenomena arising from a simple underlying discrete dynamics. If correct, this perspective may represent a significant shift in our understanding of fundamental physics.

Final Remarks

Whether nature is fundamentally discrete remains an empirical question. The framework presented here demonstrates that such discreteness, if present, is sufficient to reproduce all currently known fundamental physical laws within a single coherent theoretical structure. Future observations will ultimately decide whether this possibility is realized in nature.

12 References and Code Availability

Code, Figures, and Reproducibility

All numerical scripts, symbolic calculations, and final figures associated with this work are made publicly available in a dedicated GitHub repository. The repository contains:

- Scripts used to analyze lattice dispersion relations and suppression of fermion doublers.
- Numerical diagnostics for projected fermion spectra and residual amplitudes.
- Cosmological evolution scripts illustrating the bounce and geometric inflation.
- Source files for all figures included in this paper.

The repository is intended to ensure full transparency and reproducibility of the results presented here and to facilitate further exploration of the discrete lattice framework by the community.

The Github repositary : https://github.com/berjarry71/discrete-unification-physics

References

References

[1] K. G. Wilson, "Confinement of Quarks," *Phys. Rev. D* **10**, 2445 (1974).

[2] T. Regge, "General Relativity Without Coordinates," *Nuovo Cimento* **19**, 558 (1961).

[3] H. B. Nielsen and M. Ninomiya, "No-Go Theorem for Regularizing Chiral Fermions," *Phys. Lett. B* **105**, 219 (1981).

[4] C. Rovelli and L. Smolin, "Spin Networks and Quantum Gravity," *Phys. Rev. D* **52**, 5743 (1995).

[5] A. Ashtekar and J. Lewandowski, "Quantum Theory of Geometry I: Area Operators," *Class. Quant. Grav.* **14**, A55 (1997).

[6] T. Thiemann, *Modern Canonical Quantum General Relativity*, Cambridge University Press (2007).

[7] M. Bojowald, "Loop Quantum Cosmology," *Living Rev. Relativity* **8**, 11 (2005).

[8] G. Amelino-Camelia et al., "Tests of Quantum Gravity from Observations of Gamma-Ray Bursts," *Nature* **393**, 763 (1998).

[9] Planck Collaboration, "Planck 2018 Results. VI. Cosmological Parameters," *Astron. Astrophys.* **641**, A6 (2020).

[10] LHAASO Collaboration, Constraints on Lorentz invariance violation from GRB 221009A, arXiv:2508.00656 (2025).